Statistical evaluation of tolerances used in frameless cranial stereotactic radiosurgery using optical surface imaging and an anthropomorphic MAX-HD SRS phantom.

Michael J Tallhamer M.Sc., Centura Health, Parker, CO

Introduction: Intracranial stereotactic radiosurgery (SRS) has traditionally relied on rigorous forms of cranial immobilization in order to deliver an accurate conformal dose of radiation to the intracranial target(s) while maintaining a sharp precipitous falloff outside of the target in the surrounding healthy tissues. Traditionally this has been accomplished with conventional stereotactic headframes which employ a couch mounted frame secured to the skull with screws through 4 supporting posts. However, in recent years many frameless options have been investigated in conjunction with a variety of x-ray and video based imaging systems allowing for accurate localization of intracranial targets with a higher degree of comfort over the more traditional and invasive frames. These systems are less invasive but often require monitoring of the patient position relative to isocenter throughout the treatment to ensure the target localization remains within the TG-142 recommended mechanical tolerances of 1mm for SRS and/or the end-to-end tolerance of 0.95 listed in TG-135. Many of these frameless SRS systems use x-ray imaging to monitor the localization of the target throughout treatment using boney landmarks to periodically evaluate the quality of the localization over time. With the advent of optical surface monitoring systems, this monitoring can happen in near real-time using a video based tracking system instead of the more traditional "point in time" x-ray based systems. However, these optical monitoring systems are uniquely decoupled from the delivery system in ways that x-ray based correction systems are not and require special validation as noted in TG-147. A number of investigations have validated the accuracy, stability, and 6D tracking capabilities of these optical tracking systems for use in SRS cases using a variety of phantoms. However, these studies often focus on simple or limited geometries using either anthropomorphic or standard geometric based phantoms generalizing the results to all patient setups, and delivery techniques which is not always as straight forward for these optical systems when dealing with rotating couch geometries, camera obstructions during portions of the treatment, various relative isocenter locations, and a variety of patient setup complications. This white paper describes a variety of end-to-end tests used to evaluate these optical systems under a wide range of treatment conditions while seeking to isolate some of the confounding variables within the optical field of view of the treatment so that a statistically realistic view of the system can be obtained. All tests were completed using either the geometric isocenter calibration phantom provided by Vision RT with the AlignRT surface guided radiation therapy (SGRT) system and/or the anthropomorphic Integrated Medical Technologies (IMT) MAX-HD head phantom for comparison. Comparisons between the phantoms and conditions are made in order to isolate the variables being discussed and to glean insight from the measurement statistics as they relate to the TG-142 and TG-147 tolerances under those conditions.

Phantoms:

The MAX-HD SRS phantom is a sectioned anthropomorphic head phantom made from tissue-equivalent materials that provide tissue attenuation values within 1% of actual attenuation from 50 keV to 25 MeV, and bone from 50 keV to 15 MeV which allow for realistic dose measurements in and around

cranial and spinal structures of interest. Within the various sections of the Max-HD, a variety of inserts can be placed to test localization capabilities, measure dose distributions using film, and acquire chamber based measurements of plans transferred to the phantom through the treatment planning system (TPS). The phantom materials simulate a variety of intracranial structures like brain, bone, oral and sinus cavities, and teeth. More importantly to this series of tests it also provides realistic cranial vault dimensions for placement of isocenters at extreme locations within the cranial vault for performance evaluation purposes as well as a Winston-Lutz insert for correlation to true radiographic isocenter and cross referencing to other phantoms. The phantom surface is also very similar to that of the isocenter calibration cube provided by Vision RT which serves to eliminate surface monitoring variations associated with poor surface texture and/or color seen in other anthropomorphic phantoms.

The isocenter calibration cube supplied by Vision RT with the AlignRT SRS capable SGRT system is a 15cm x 15cm x 15cm cube phantom formed from a solid machined polystyrene with 5 x 7.5mm diameter aluminum ceramic spheres embedded within it. One of these spheres is located in the exact center of the cube, the other four are arranged asymmetrically about the central sphere within the cube. The Vision RT Isocenter Calibration Software allows AlignRT to be directly calibrated to the treatment isocenter using a Winston-Lutz type process which has been shown to remove any calibration bias introduced during the monthly calibration process. The 5 visible surfaces of the phantom have an engraved line to aid positioning with respect to the light field of the treatment delivery system, and / or room lasers. The manufacturer states that the color and finish of external surface of the cube allows the phantom to be imaged easily by AlignRT.

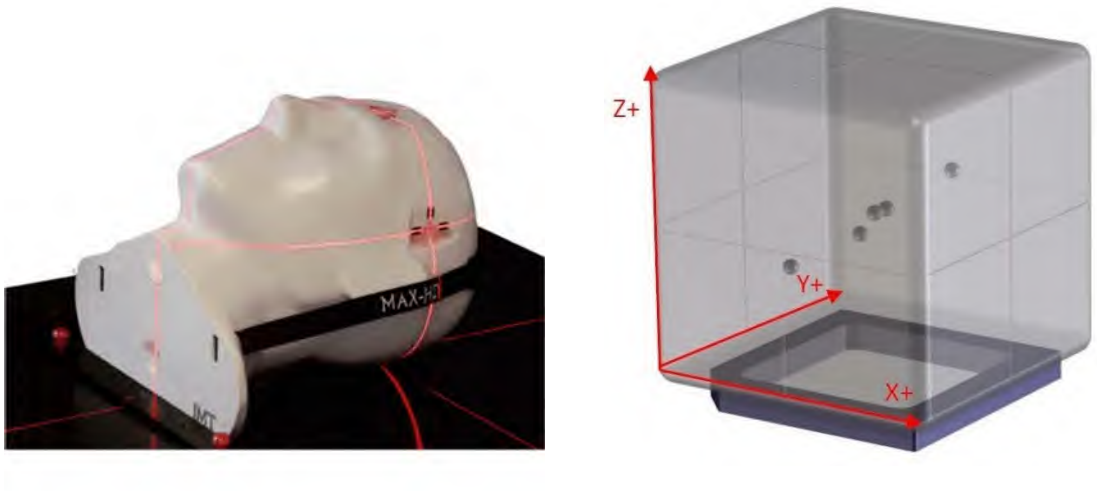

Figure 1: Integrated Medical Technologies (IMT) MAX-HD SRS head phantom (left), Vision RT isocenter calibration phantom (right)

CT Simulation and Treatment Planning:

Both phantoms were CT simulated using our standard Intracranial SRS protocol and pushed to the treatment planning system (TPS) for segmentation, surface definition, and planning. The MAX-HD was CT simulated in 3 different anatomical positions replicating simulations with requested chin up

(MAX-HD_U), chin down (MAX-HD_D), and head neutral (MAX-HD_N). The MAX-HD was also simulated in the head neutral position with and without an Orfit 3 Point Hybrid Open Face thermoplastic mask to allow for investigation of the effects of the mask material on the localization and real-time monitoring of the phantom. Figure 2 below shows the 3 anatomical positions used for testing with the MAX-HD.

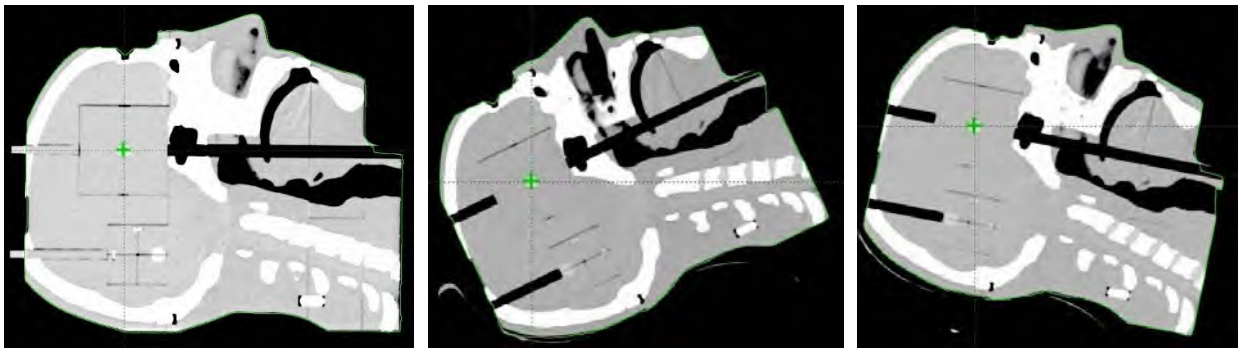

(a) (b) (c)

Figure 2: MAX-HD SRS head phantom CT simulated in 3 anatomical position (a) Head Neutral (b) Chin Up (c) Chin Down

The Varian Eclipse TPS was used to place a series of plans with isocenters at the extents of the MAX-HD_N cranial vault in the neutral head position scans ((a) from Figure 2 above). The isocenters were placed relative to the central location of the Winston-Lutz marker with the marker denoted by the position name ***Center***. An imaging plan was created at each isocenter placed at the extreme superior (**Sup**), inferior (**Inf**), right (**RtLat**), left (**LtLat**), anterior (**Ant**), and posterior (**Post**) locations within the cranial vault of the MAX-HD (see **Figure 3** below). The CT data sets for both the chin up (MAX-HD_{UP}) and chin down (MAX-HD_{DOWN}) scans were then fused to the MAX-HD_N scan and the isocenters were then transferred to the respective scans maintaining each isocenter's relative anatomical position to the body surface and location within the cranial vault.

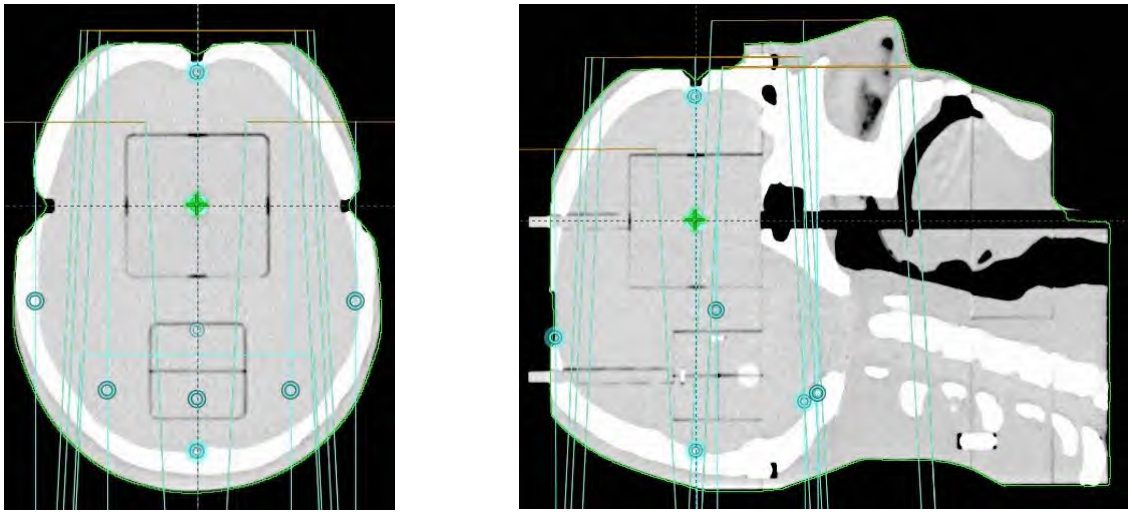

Figure 3: Isocenter locations within the MAX-HD SRS head phantom (cyan circles)

For the Vision RT isocenter calibration cube data set, imaging plans with numbered isocenters were placed in each of the 7.5mm aluminum spheres. The isocenter numbering followed the numbering

scheme from the ***Vision RT Calibration Phantom Users Guide*** increasing from 1 to 5 as one traverses from the front face to the back face with isocenter 3 being placed in the central sphere. Individual MLC based Winston-Lutz plans were placed at the central location on each data set (***Central*** isocenter on the MAX-HD and isocenter ***3*** within the Vision RT calibration phantom) for absolute radiographic verification of the target location with couch rotation for comparison to the optical tracking statistics obtained with Align RT during testing.

Once planning was complete all plans were exported to DICOM compatible format and transferred to the TrueBeam in order to run the plans in Machine QA mode. All DICOM plans and structure sets were also exported to AlignRT for import and ROI creation. It should be noted that ROIs were generated once and then imported into all the additional datasets for each respective phantom much in the same way the isocenters were generated once and transferred through fusion to the subsequent datasets to ensure that the ROI size and location relative to the isocenter was exactly the same for all isocenter to avoid the possibility of ROI differences being the cause of any discrepancies seen during measurement.

Measurements:

All measurements were performed on a Varian TrueBeam® v2.5 MR1 (IEC 61217 scale) with the Perfect Pitch 6DoF couch, HDMLC, and Align RT v5.0.1749 (Neasden). AlignRT's monthly calibration was completed using the vendors raised plate calibration technique and then corrected to isocenter using the isocenter calibration phantom and Vision RT's Isocenter Calibration Software. Measurements spanned many days taking on average 1.5 – 2.0 hours per session. Each set of measurements were comprised of 15 individual 3-5 minute long static sampling measurements using the ***Mid*** skin tone setting in AlignRT under constant ambient room lighting. Data from each measurement was plotted in a probability plot to verify the data conformed to a normal distribution then used to generate normalized histograms and fit to a normalized probability distribution. Measurements were made at 7 different couch rotations (90, 60, 30, 0, 330, 300, 270) spanning the full range of motion for the Perfect Pitch couch with an open field of view for all three cameras. As part of the same set of measurements an additional set of measurements were repeated at each couch angle with gantry angles of 45 (couch 270, 300, 330, 0) and 315 (couch 90, 60, 30, 0) degrees in order to completely block camera pods 1 and 2 respectively to establish the effect of camera obstruction during delivery at these couch positions. Each set of measurements once started were completed in one session under a single setup to avoid confounding variables within the statistics spanning separate setups. The morning QA procedure was performed daily with all reported RMS errors <0.2mm over the period the measurements were taken.

Before any measurements were completed preliminary evaluation of both the imaging system, couch and AlignRT were performed. Varian IsoCal verification was performed prior to imaging each session to verify that the imaging system was calibrated and within 0.1mm of baseline. A Winston-Lutz test using the CBCT imaging system and the Perfect Pitch couch for 6DoF alignment was run on both the Winston-Lutz marker in the MAX-HD_N data set and the central 7.5mm aluminum ceramic sphere in the Vision RT isocenter calibration phantom. Both Winston-Lutz tests showed the 3D target position had <0.2mm maximum deviation in any one translational direction from radiographic isocenter post CBCT

alignment. A second set of Winston-Lutz tests were completed using only the AlignRT system for localization to evaluate the localization capabilities of AlignRT alone on each of the phantoms. The results showed that the deviation from CBCT localization was <0.2mm in any one direction with the greatest discrepancy in the vertical direction on both phantoms. These Winston-Lutz results were verified by both commercially available and in-house software prior to starting measurements at any of the planned isocenters.

Test 1: Phantom Surface Performance (Skin tone effects on monitoring statistics)

After the mechanical and imaging stability of the system was established statistical evaluation of the system began with evaluation of the skin tone settings within AlignRT. The stationary MAX-HD was monitored using the DICOM reference surface on the MAX-HD_N data set after CBCT alignment using each of the skin tone settings within Align RT. The result shown in Figure 4 show that the various skin tone settings had minimal effect on the systematic offset when their normalized distributions were compared over time. The means of 0.019cm, 0.018cm, 0.018cm for the Fair, Mid, and Dark settings respectively show a similar systematic offset from the DICOM reference surface to the final CBCT localized position. The random error in the measurements was relatively small compared to the systematic error with standard deviations of 0.003 for all three settings. The total vector displacement (magnitude ***MAG*** in the AlignRT software) was chosen as the measurement to represent quality of the overall localization. Where larger deviations were seen in subsequent tests the constituents of the vector displacement were examined to determine if one dimension was the primary cause of the difference or if all dimensions played a role in the discrepancy from the reference surface. All mean rotational offsets were held under 0.04 degrees at the single static couch angle. These values compared very favorably to the original commissioning data completed on the Vision RT isocenter calibration phantom with those distribution means measuring 0.015cm, 0.014cm, 0.015cm for the Fair, Mid, and Dark settings respectively and rotational offsets held below 0.03 degrees. This indicates that the two phantom surfaces perform similarly under the same experimental conditions and should not introduce significant statistical error in future tests.

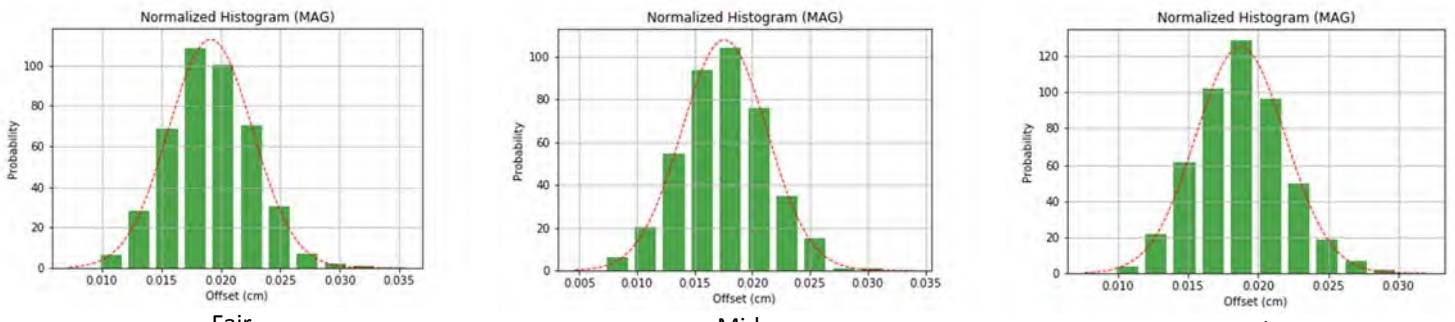

Figure 4: Normalized distributions for Fair, Mid, and Dark skin tone settings respectively. Red line represents fit to a normalized probability distribution.

Test 2: Reference Surface Performance (Reference surface statistics at various isocenter locations)

With the first test complete the decision was made to use the Mid skin tone setting for all subsequent measurements. The next test performed was intended to verify the performance of the different types of reference surfaces at different isocenter locations within the MAX-HD_N. We first determined the systematic offset of the DICOM surface generated in the TPS from the final CBCT localized position for each isocenter position using the MAX-HD_N data set. Previous commissioning using the isocenter calibration phantom provided with the AlignRT system resulted in a systematic offset of -0.0105cm, 0.015cm, -0.029cm in the VRT, LAT, and LNG dimensions respectively when aligned to the central isocenter (isocenter number 3). Reference surface performance was not evaluated at additional isocenters during the original commissioning. These values were confirmed under the monitoring conditions of this current work (CUBE measurements in Figure 5 below) and plotted against the values obtained at each of the MAX-HD_N isocenters. Analysis of the DICOM surface results after CBCT alignment showed a spreading of these values with isocenter location within the cranial vault on the MAX-HD_N which we had not seen using the isocenter calibration phantom with the isocenter located at its central position. The VRT, LAT, LNG, and MAG plots in Figure 4 below show a trend where deviations from the DICOM reference surface used for monitoring to final CBCT position increase as the orthogonal distance to the monitoring surface plane increases. The LAT plot below shows an interesting lateral offset of the RTLAT isocenter location that should warrant further investigation using the symmetrically located LTLAT isocenter not reported on in this work. All rotational degrees of freedom were held to a mean 0.009 degrees (range -0.11-0.14 degrees)

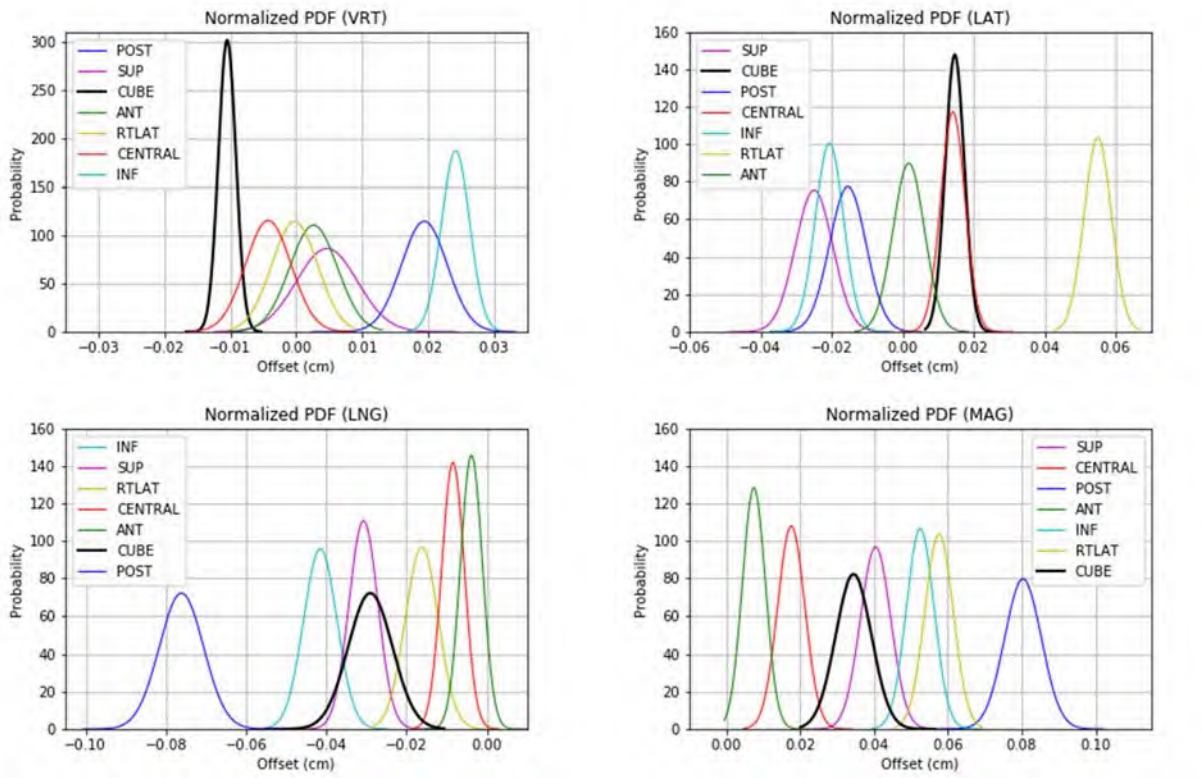

Figure 4: Normalized probability distributions for the 3 translational degrees of freedom and the magnitude of the total vector displacement reported after CBCT alignment to each of the isocenters within the MAX-HD_N.

Performing this same test using an AlignRT reference surface of the MAX-HD_N acquired after CBCT positioning shows a convergence toward 0.0cm offset as one would expect. The POST isocenter location remains an outlier as can be seen from the MAG plot in Figure 5 below but is still within the SRS tolerance of 1mm/0.5degrees. You can also see that all dimensions for the POST isocenter are represented by broader normalized distributions indicating more noise in the readings. After reference surface acquisition the systematic offset of the MAG for all isocenters, with the exception of the POST isocenter (mean 0.0218cm), remained below 0.01cm (range 0.0047 – 0.0083) for monitoring at a couch rotation of 0 degrees. Re-acquiring the POST isocenter reference image did not change the measurement distribution characteristics. Again, all rotational degrees of freedom were held to a mean of 0.003 degrees (range -0.10-0.11 degrees)

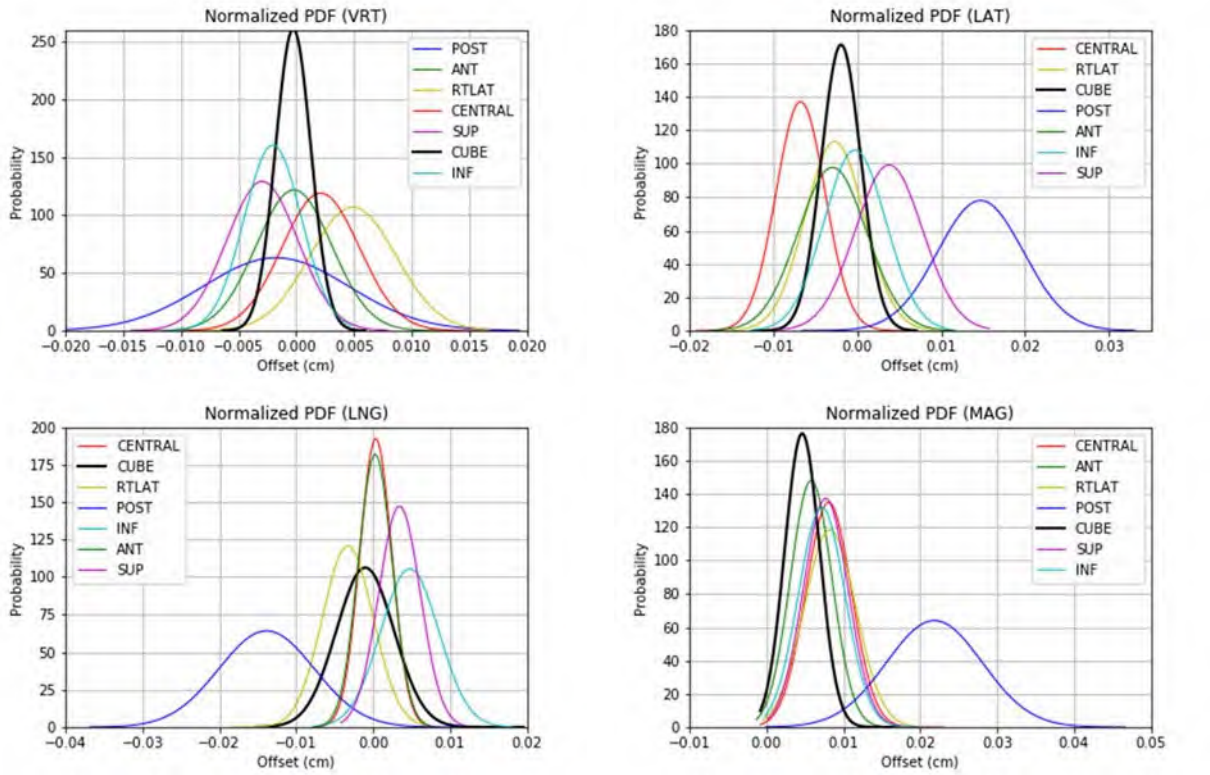

Figure 5: Normalized probability distributions for the 3 translational degrees of freedom and the magnitude of the total vector displacement reported after acquiring an AlignRT reference image for monitoring post CBCT alignment to each of the isocenters within the MAX-HD_N.

Test 3: Camera Obstruction Effects on Reference Surface Statistics

Camera obstruction measurements were obtained while maintaining the setups from the above tests. In an effort to isolate the effect of camera obstruction from other variables the obstruction measurements were obtained in sequence immediately after the measurements from Test 2 without disturbing the setup or ambient room conditions. With the couch still at the approved CBCT localization position, the side camera pods were obstructed using the gantry to simulate an obstruction during delivery. Gantry angles of 45 and 315 were used to completely block camera pods 1 and 2 respectively while monitoring the MAX-HD_N with the AlignRT reference surface acquired after CBCT localization. As

can be seen in Figure 6 below the effects of the camera obstruction, while small and statistically insignificant in most cases, vary with the camera pod obstructed and the location of isocenter within the phantom.

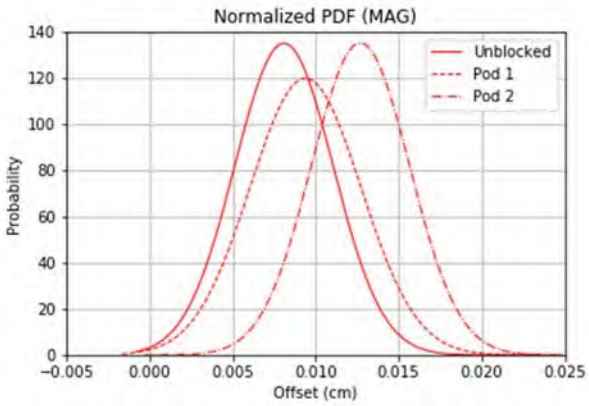

(CENTRAL)

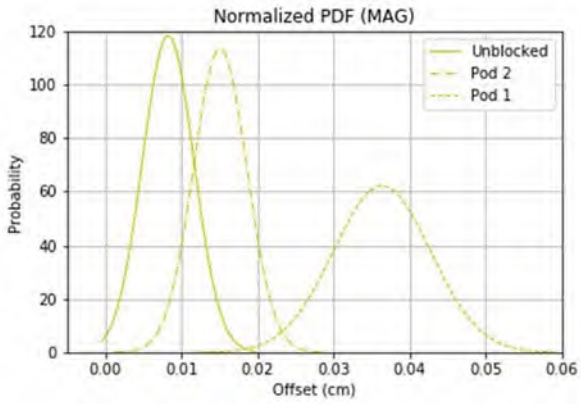

(RTLAT)

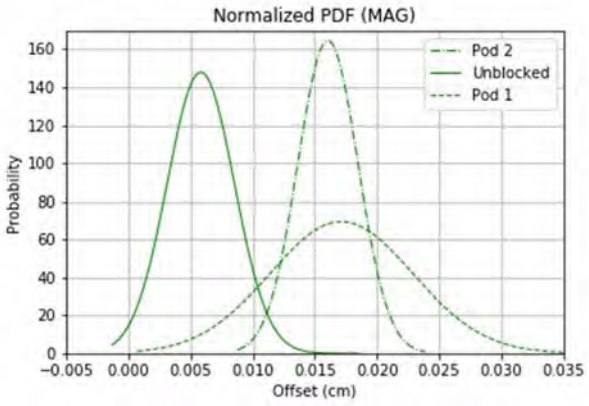

(ANT)

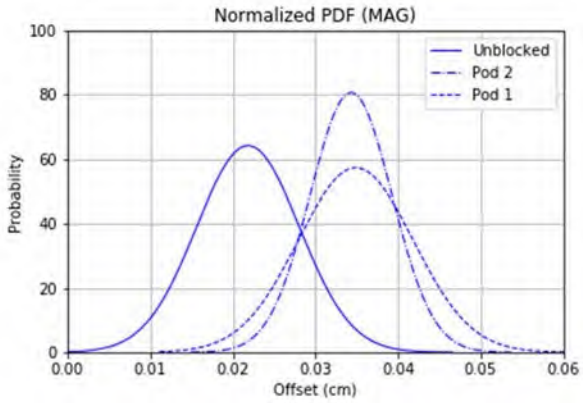

(POST)

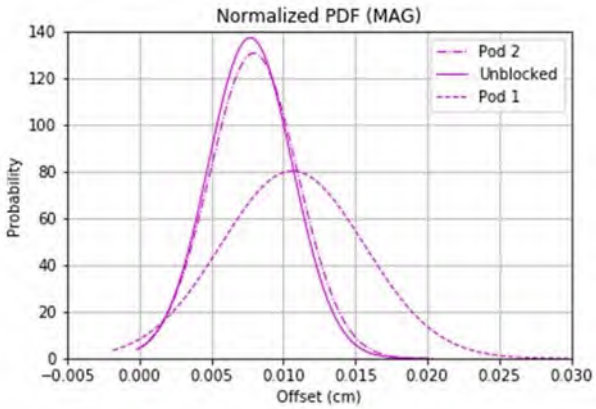

(SUP)

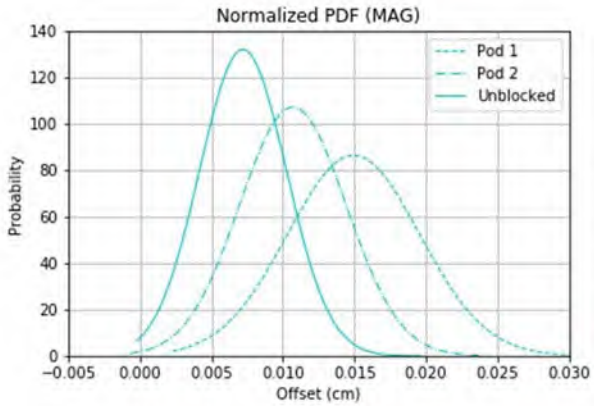

(INF)

Figure 6: Normalized probability distributions for the magnitude of the total vector displacement reported after obstructing the camera pods during monitoring using an AlignRT reference image for monitoring post CBCT alignment to each of the isocenters within the MAX-HD$_N$.

Mean differences ranging from 0.0002cm (within the noise of the system) to 0.0281cm for the RTLAT isocenter location were observed during camera obstruction. It should be noted that again the POST isocenter showed a change in mean position larger than those observed for the other isocenter locations. The RTLAT isocenter location saw a significant change in the mean position when camera pod 1 was obstructed by the gantry. This pod represents the pod closes to the offset position of the isocenter so the primary monitoring of the phantom was accomplished using the unblocked pods 2 and 3 of the AlignRT system which are farther away from the surface being monitored. Further investigation into this observation will have to be completed using a symmetrically placed isocenter in the left lateral aspect of the cranial vault of the MAX-HD$_N$ data set to see if an equal but opposite effect is seen when the phantom is offset in the opposite direction. The rotational degrees of freedom in this test as before remained stable under obstruction of the various camera pods with a combined mean of 0.004 degrees and range of -0.11 – 0.15 degrees

Isocenter	Pod	Mean	Ref Mean	Difference
CENTRAL	1	0.0094	0.0081	0.0013
CENTRAL	2	0.0127	0.0081	0.0046
RTLAT	1	0.0364	0.0083	0.0281
RTLAT	2	0.0151	0.0083	0.0068
ANT	1	0.0171	0.0058	0.0113
ANT	2	0.0160	0.0058	0.0102
SUP	1	0.0106	0.0077	0.0029
SUP	2	0.0079	0.0077	0.0002
INF	1	0.0149	0.0072	0.0077
INF	2	0.0107	0.0072	0.0035
POST	1	0.0349	0.0218	0.0130
POST	2	0.0343	0.0218	0.0125

Table 1: Summary of mean shifts during monitoring while obstructing the camera pods as a function of isocenter location.

Test 4: Couch Angle Effects on Reference Surface Statistics

Couch rotational effect on the real-time delta values have been reported to our institution on a number of occasions. In order to test these effects on the real-time delta values we again sampled the MAX-HD$_N$ at 7 different couch positions typically used in our intracranial SRS programs. The MAX-HD$_N$ was positioned at one of seven predetermined couch values (0, 30, 60, 90, 270, 300, and 330 degrees) and monitored with the AlignRT reference surface obtained after CBCT localization at couch 0. The couch angles were entered into the AlignRT software manually and the reference surface adjusted through the software to match the desired angle. All couch corrections from the CBCT including pitch roll and rotation were maintained throughout the full range of couch angles. At each couch angle the central fiducial of the Winston-Lutz insert was imaged using the portal imaging system prior to monitoring to verify expected couch walkout against the pretesting Winston-Lutz values. Measurement means were not corrected for couch walkout at the CENTRAL isocenter location since there wasn't a systematic way to do this across all isocenter locations without a Winston-Lutz target.

MAX_HD$_N$ (VRT)												
	CENTRAL		POST		ANT		SUP		INF		RTLAT	
Couch	Open	Blocked	Open	Blocked	Open	Blocked	Open	Blocked	Open	Blocked	Open	Blocked
0	0.002	-0.004	-0.002	0.001	0.000	-0.005	-0.003	-0.001	-0.002	-0.004	0.005	0.013
30	-0.012	-0.014	-0.014	-0.010	-0.027	-0.013	-0.021	-0.031	-0.020	-0.027	-0.004	-0.006
60	-0.016	-0.017	-0.020	-0.009	-0.007	0.008	-0.005	-0.002	-0.020	-0.021	0.000	0.004
90	-0.007	-0.010	-0.002	0.000	0.008	-0.001	-0.001	-0.007	-0.015	-0.010	0.006	0.005
270	0.002	0.003	-0.009	0.003	0.000	0.003	-0.001	0.004	-0.016	-0.010	-0.005	-0.002
300	0.000	-0.003	-0.004	-0.011	-0.006	0.004	-0.010	-0.008	-0.015	-0.014	0.005	-0.006
330	0.003	-0.003	-0.005	-0.012	-0.014	0.001	-0.013	-0.025	-0.009	-0.017	0.027	0.007

MAX_HD$_N$ (LAT)												
	CENTRAL		POST		ANT		SUP		INF		RTLAT	
Couch	Open	Blocked	Open	Blocked	Open	Blocked	Open	Blocked	Open	Blocked	Open	Blocked
0	-0.007	-0.005	0.015	0.021	-0.003	0.009	0.004	0.003	0.000	0.002	-0.003	-0.005
30	0.016	0.013	0.036	0.043	0.032	0.015	0.012	0.025	0.038	0.043	0.007	0.007
60	0.016	0.013	0.052	0.052	0.010	0.002	0.028	0.029	0.047	0.041	0.017	0.020
90	-0.015	-0.014	-0.007	0.007	-0.036	**-0.065**	0.027	0.013	-0.002	-0.018	-0.014	-0.016
270	0.022	0.022	**0.077**	**0.065**	**0.067**	**0.079**	0.017	0.017	0.033	0.024	0.011	0.009
300	0.037	0.045	**0.072**	**0.074**	0.050	**0.066**	0.053	0.055	0.043	0.053	0.028	0.035
330	-0.001	-0.002	0.019	0.030	-0.002	0.006	0.027	0.019	0.007	0.014	-0.004	-0.004

MAX_HD$_N$ (LNG)												
	CENTRAL		POST		ANT		SUP		INF		RTLAT	
Couch	Open	Blocked	Open	Blocked	Open	Blocked	Open	Blocked	Open	Blocked	Open	Blocked
0	0.000	0.000	-0.014	-0.025	0.000	-0.012	0.003	0.005	0.005	0.008	-0.003	-0.004
30	-0.018	-0.022	-0.047	**-0.066**	0.017	0.012	-0.020	-0.024	-0.009	-0.016	-0.016	-0.011
60	-0.045	-0.044	**-0.063**	-0.056	-0.011	-0.018	-0.022	-0.023	0.014	-0.006	-0.031	-0.018
90	-0.048	-0.049	-0.042	-0.045	-0.014	-0.032	-0.015	-0.029	0.011	0.018	-0.039	-0.060
270	-0.029	-0.024	-0.043	-0.023	-0.008	-0.020	-0.012	-0.010	0.018	0.038	-0.009	-0.009
300	-0.026	-0.029	-0.030	-0.033	0.000	0.006	-0.023	-0.025	0.002	0.002	0.011	0.004
330	-0.019	-0.029	-0.055	**-0.063**	0.019	0.009	-0.020	-0.039	-0.028	-0.035	0.016	-0.003

MAX_HD$_N$ (MAG)												
	CENTRAL		POST		ANT		SUP		INF		RTLAT	
Couch	Open	Blocked	Open	Blocked	Open	Blocked	Open	Blocked	Open	Blocked	Open	Blocked
0	0.008	0.011	0.022	0.035	0.006	0.016	0.008	0.008	0.007	0.011	0.008	0.015
30	0.028	0.030	**0.061**	**0.080**	0.045	0.024	0.032	0.047	0.045	0.054	0.019	0.015
60	0.050	0.049	**0.084**	**0.077**	0.017	0.020	0.037	0.038	0.053	0.047	0.036	0.028
90	0.051	0.052	0.043	0.046	0.039	**0.073**	0.032	0.034	0.020	0.028	0.043	**0.063**
270	0.037	0.033	**0.089**	**0.069**	**0.068**	**0.082**	0.023	0.021	0.041	0.046	0.017	0.015
300	0.046	0.054	**0.078**	**0.082**	0.050	**0.067**	0.059	**0.061**	0.046	0.055	0.031	0.036
330	0.019	0.030	0.059	**0.071**	0.024	0.012	0.037	0.050	0.031	0.042	0.032	0.011

Table 2: Systematic shift of the Max-HD$_N$ at various couch angles with and without obstructing the camera pods as a function of isocenter location. Bold red values indicate offsets of 0.06cm or greater as an indication where more than half of our 1mm/0.5degree tolerance for SRS is accounted for in just the statistical offset.

The MAX-HD$_N$ was then monitored with both an open camera arrangement and an obstructed camera arrangement identical to the arrangement described in the Test 3. The results for 6 MAX-HD$_N$ Isocenters across all couch angles are summarized in Table 2 above. The mean position of the normal distribution is

reported in the table and represents the systematic offset of the data at each couch position and isocenter combination. All reference surfaces were taken at couch 0. As before all sample data was normalized, plotted in a probability plot, and fit to a normal distribution to verify the sampling statistics.

	MAX_HD$_N$ (VRT)				Calibration Cube (VRT)			
	CENTRAL		POST		CENTRAL		POST	
Couch	Open	Blocked	Open	Blocked	Open	Blocked	Open	Blocked
0	0.002	-0.004	-0.002	0.001	0.000	0.003	0.006	0.017
30	-0.012	-0.014	-0.014	-0.010	0.001	0.003	0.003	0.009
60	-0.016	-0.017	-0.020	-0.009	0.001	0.004	0.015	0.020
90	-0.007	-0.010	-0.002	0.000	-0.002	0.003	0.014	0.018
270	0.002	0.003	-0.009	0.003	0.004	0.008	0.023	0.030
300	0.000	-0.003	-0.004	-0.011	0.006	0.008	0.022	0.023
330	0.003	-0.003	-0.005	-0.012	0.003	0.001	0.017	0.020

	MAX_HD$_N$ (LAT)				Calibration Cube (LAT)			
	CENTRAL		POST		CENTRAL		POST	
Couch	Open	Blocked	Open	Blocked	Open	Blocked	Open	Blocked
0	-0.007	-0.005	0.015	0.021	-0.002	-0.003	0.009	0.042
30	0.016	0.013	0.036	0.043	0.031	0.020	0.024	0.030
60	0.016	0.013	0.052	0.052	0.031	0.013	0.031	0.025
90	-0.015	-0.014	-0.007	0.007	-0.009	-0.007	0.007	0.021
270	0.022	0.022	**0.077**	**0.065**	0.043	0.040	0.052	0.047
300	0.037	0.045	**0.072**	**0.074**	0.045	0.053	**0.072**	**0.076**
330	-0.001	-0.002	0.019	0.030	0.004	0.006	0.030	0.030

	MAX_HD$_N$ (LNG)				Calibration Cube (LNG)			
	CENTRAL		POST		CENTRAL		POST	
Couch	Open	Blocked	Open	Blocked	Open	Blocked	Open	Blocked
0	0.000	0.000	-0.014	-0.025	-0.001	0.004	-0.006	-0.019
30	-0.018	-0.022	-0.047	**-0.066**	0.017	0.029	0.001	-0.011
60	-0.045	-0.044	**-0.063**	-0.056	0.007	0.010	-0.023	-0.010
90	-0.048	-0.049	-0.042	-0.045	-0.004	0.001	-0.034	-0.024
270	-0.029	-0.024	-0.043	-0.023	0.017	0.018	-0.011	-0.004
300	-0.026	-0.029	-0.030	-0.033	0.040	0.042	0.004	0.015
330	-0.019	-0.029	-0.055	**-0.063**	0.020	0.027	-0.006	-0.006

	MAX_HD$_N$ (MAG)				Calibration Cube (MAG)			
	CENTRAL		POST		CENTRAL		POST	
Couch	Open	Blocked	Open	Blocked	Open	Blocked	Open	Blocked
0	0.008	0.011	0.022	0.035	0.005	0.007	0.014	0.049
30	0.028	0.030	**0.061**	**0.080**	0.036	0.036	0.025	0.034
60	0.050	0.049	**0.084**	**0.077**	0.032	0.017	0.042	0.034
90	0.051	0.052	0.043	0.046	0.011	0.008	0.038	0.037
270	0.037	0.033	**0.089**	**0.069**	0.047	0.045	0.058	0.056
300	0.046	0.054	**0.078**	**0.082**	**0.061**	**0.068**	**0.076**	**0.081**
330	0.019	0.030	0.059	**0.071**	0.020	0.028	0.035	0.037

Table 3: Systematic shift comparison between the MAX-HD$_N$ and the Vision RT isocenter calibration cube at 7 couch angles with and without obstructing the camera pods for 2 isocenter locations

Comparing the performance of the MAX-HD$_N$ and the isocenter calibration cube meant placing an isocenter outside of the physical cube boundaries in the TPS since the cranial vault of the MAX-HD$_N$ allows for posterior placement of isocenter beyond 15cm from the monitoring surface. This was done for the central and posterior isocenter and the data summarized in Table 3. During the original commissioning, the most posterior isocenter was placed approximately 14cm from the surface of the calibration cube along the central planes of the phantom. This location resulted in all reported differences at couch angles of 0, 45, 90, 270, and 315 degrees to be less than 0.05cm. In the current work the isocenter is place at 17.5 cm below the anterior surface of the calibration cube and run under the current experimental conditions at the 7 previously described couch angles. It can be seen from the total magnitude in Table 3 that the calibration cube still results in mean offsets less than the MAX-HD$_N$. This could be due to surface contour symmetries that exist in the isocenter calibration cube that don't in the MAX-HD but further investigation would be required to determine how much of a role these symmetries actually play. However, the MAX-HD phantom is closer to the patient geometries experienced during treatment delivery so discrepancies seen under these conditions should be considered when commissioning a system for clinical use. It should also be noted from the results in both Table 2 and Table 3 that the isocenters displaying the largest discrepancies from the reference image position were in the anterior posterior direction with the posterior isocenter representing the maximum position away from the monitoring surface within the cranial vault and the anterior iso representing the closest point to the monitoring surface while still within the cranial vault. This supports

the idea that the random speckle pattern projected on the surface of the patient by the AlignRT cameras is optimized and/or focused to give optimal performance to a surface within a given distance from isocenter. Another interesting observation is that the vertical displacement under these experimental conditions appears to be very stable while the primary contributors to the deviations in the magnitude come from both the lateral and longitudinal delta measurements during the couch rotation. This is consistent with other reports made to our institution but to what extent is hard to determine given no measurements were provided. Under all measurement conditions the system was able to maintain the 1mm/0.5 degree SRS tolerances used for clinical treatments consistent with the previous commissioning data obtained when the machine was installed.

Images at various couch position were reviewed to determine if there were potentially field of view issues that might be contributing to the discrepancy in the real-time delta values with changes in isocenter location and couch rotation. It was found that for some couch rotations and isocenter combinations the region of interest for monitoring was clipped. Figure 7 below illustrates the field of view clipping on the imaging sensor for the posterior isocenter during monitoring at couch angle 300.

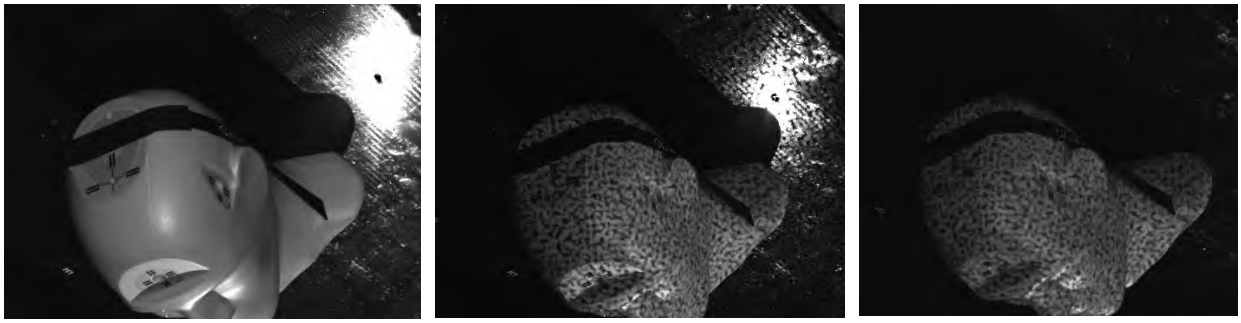

Figure 7: Texture and speckle images from Pod 1 taken at the POST isocenter location and couch angle 300 degrees on the MAX-HD_N showing clipping at the edge of the imaging sensor that cuts through the ROI.

Test 5: Gross Anatomical Positioning Effects on Reference Surface Statistics

With the couch angle and isocenter location data completed the next test was designed to isolate the effects of anatomical positioning on the cameras ability to accurately monitor the phantom position under identical setup conditions as previously described. For the purpose of this white paper we will limit the reported results to both the central and posterior isocenters as they seem to illustrate the extremes of what might be encountered during the clinical application of SGRT for intracranial SRS. The MAX-HD was monitored at the central and posterior isocenters with the MAX-HD_N, MAX-HD_U, and MAX-HD_D data sets to determine if the relative orientation of the monitoring surface effected the reference surface monitoring statistics. Table 4 summarizes the results of these measurements. It can be seen that the mean offsets with the MAX-HD_U data set are marginally worse than the MAX-HD_N data set while the MAX-HD_D data set out performs the previous 2 and is comparable (or marginally better) than the Vision RT isocenter calibration cube when compared to the data in Table 3. The MAX-HD_U data set exceeded the 1mm tolerance for SRS at the couch angle of 300 degrees and represents the only condition where a tolerance was exceeded in this current work. All rotational degrees of freedom remained below 0.3 degrees at all positions

	MAX_HD$_N$ (VRT)				MAX_HD$_U$ (VRT)				MAX_HD$_D$ (VRT)			
	CENTRAL		POST		CENTRAL		POST		CENTRAL		POST	
Couch	Open	Blocked	Open	Blocked	Open	Blocked	Open	Blocked	Open	Blocked	Open	Blocked
0	0.002	-0.004	-0.002	0.001	0.002	0.011	0.011	0.020	0.002	-0.001	0.000	-0.002
30	-0.012	-0.014	-0.014	-0.010	0.025	0.024	-0.011	-0.005	-0.008	-0.009	-0.003	-0.014
60	-0.016	-0.017	-0.020	-0.009	0.027	0.026	-0.019	-0.018	-0.007	0.001	-0.001	0.002
90	-0.007	-0.010	-0.002	0.000	0.029	0.024	-0.018	-0.017	0.002	-0.005	-0.001	0.002
270	0.002	0.003	-0.009	0.003	0.023	0.016	0.017	0.039	-0.001	-0.008	-0.015	0.002
300	0.000	-0.003	-0.004	-0.011	0.017	0.015	0.022	0.022	-0.006	0.000	0.004	0.005
330	0.003	-0.003	-0.005	-0.012	0.021	0.022	0.021	0.034	0.000	0.007	-0.001	0.000

	MAX_HD$_N$ (LAT)				MAX_HD$_U$ (LAT)				MAX_HD$_D$ (LAT)			
	CENTRAL		POST		CENTRAL		POST		CENTRAL		POST	
Couch	Open	Blocked	Open	Blocked	Open	Blocked	Open	Blocked	Open	Blocked	Open	Blocked
0	-0.007	-0.005	0.015	0.021	0.001	0.000	0.011	0.006	0.000	-0.001	-0.006	-0.006
30	0.016	0.013	0.036	0.043	0.035	0.033	0.011	0.001	0.028	0.027	0.019	0.030
60	0.016	0.013	0.052	0.052	0.021	0.020	0.002	-0.016	0.028	0.022	0.055	0.045
90	-0.015	-0.014	-0.007	0.007	0.004	-0.005	0.033	0.024	0.005	0.002	-0.033	-0.013
270	0.022	0.022	**0.077**	**0.065**	0.040	0.051	**0.064**	0.060	0.039	0.040	0.041	0.034
300	0.037	0.045	**0.072**	**0.074**	0.051	**0.072**	**0.083**	**0.109**	0.052	0.058	0.028	0.030
330	-0.001	-0.002	0.019	0.030	0.015	0.010	0.022	0.043	0.006	0.004	0.016	0.013

	MAX_HD$_N$ (LNG)				MAX_HD$_U$ (LNG)				MAX_HD$_D$ (LNG)			
	CENTRAL		POST		CENTRAL		POST		CENTRAL		POST	
Couch	Open	Blocked	Open	Blocked	Open	Blocked	Open	Blocked	Open	Blocked	Open	Blocked
0	0.000	0.000	-0.014	-0.025	0.007	-0.003	-0.004	-0.020	0.001	-0.015	0.008	0.010
30	-0.018	-0.022	-0.047	**-0.066**	-0.014	-0.025	0.014	-0.024	-0.019	-0.019	-0.007	-0.010
60	-0.045	-0.044	**-0.063**	-0.056	-0.043	-0.038	**0.062**	0.013	-0.032	-0.029	-0.017	-0.015
90	-0.048	-0.049	-0.042	-0.045	-0.032	-0.040	**0.072**	**0.080**	-0.044	-0.046	-0.023	-0.019
270	-0.029	-0.024	-0.043	-0.023	0.008	-0.010	0.046	0.019	-0.031	-0.042	-0.044	-0.023
300	-0.026	-0.029	-0.030	-0.033	0.010	-0.013	0.031	-0.006	-0.024	-0.024	-0.005	-0.006
330	-0.019	-0.029	-0.055	**-0.063**	-0.004	-0.030	-0.003	-0.041	-0.024	-0.025	-0.029	-0.024

	MAX_HD$_N$ (MAG)				MAX_HD$_U$ (MAG)				MAX_HD$_D$ (MAG)			
	CENTRAL		POST		CENTRAL		POST		CENTRAL		POST	
Couch	Open	Blocked	Open	Blocked	Open	Blocked	Open	Blocked	Open	Blocked	Open	Blocked
0	0.008	0.011	0.022	0.035	0.009	0.021	0.017	0.032	0.005	0.016	0.011	0.015
30	0.028	0.030	**0.061**	**0.080**	0.045	0.048	0.022	0.026	0.035	0.035	0.021	0.035
60	0.050	0.049	**0.084**	**0.077**	0.055	0.051	**0.066**	0.029	0.043	0.037	0.058	0.048
90	0.051	0.052	0.043	0.046	0.044	0.047	**0.081**	**0.086**	0.045	0.047	0.041	0.024
270	0.037	0.033	**0.089**	**0.069**	0.047	0.055	**0.081**	**0.074**	0.050	0.059	**0.063**	0.042
300	0.046	0.054	**0.078**	**0.082**	0.055	**0.075**	**0.092**	**0.112**	0.058	**0.063**	0.029	0.032
330	0.019	0.030	0.059	**0.071**	0.027	0.039	0.032	**0.069**	0.025	0.027	0.034	0.029

Table 4: Systematic shift of the Max-HD at various couch angles with and without obstructing the camera pods as a function of isocenter location and head position. Bold red values indicate offsets of 0.06cm or greater as an indication where more than half of our 1mm/0.5degree tolerance for SRS is accounted for in just this statistical offset.

Texture and speckle images at the various couch positions were evaluated for both the central and posterior isocenters for all three data sets as in Test 4. Clipping was seen at a couch angle of 300 degrees for all data sets with the clipping on the MAX-HD_N data set being the worst. The head tilts in the other data sets helped to avoid the clipping to some extent but in the case of the MAX-HD_U data set that came at the cost of limiting the visibility of the ROI region via the tipping of the head away from the viewing angle of the cameras which has a similar effect of "clipping" the ROI by virtue of self-obstruction.

Test 6: ROI Overlap with Perforated Mask Effects on Reference Surface Statistics

The final test completed looked at the effects of the immobilization mask on the monitoring statistics when the ROI defined in AlignRT at the time of import propagates to both the patient and mask after CBCT localization and subsequent reference surface capture. Our Institutional procedures have been designed so that great care is taken to ensure that transferred ROIs do not overlap onto the mask during clinical use of the system to avoid potential errors in the registration of the surfaces. In order to test the effects of the mask on the monitoring statistics, the MAX-HD_N data set was simulated with and without a mask in place. The ROI defined in the AlignRT software was allowed to overlap the mask and transfer to both the MAX-HD surface as well as the mask material after CBCT localization as shown in Figure 8 below. The phantom with the mask in place and the monitoring ROI that included the mask material was then put through the same set of measurements as Test 4 at the central isocenter location. This allow a direct statistical comparison of the phantom with and without the mask in place at all couch angles using an identically sized ROI without the potential for clipping and the imaging sensor plane. This should give a directly comparable set of measurements for determining the effects of the mask alone on the monitoring statistics at each measurement position. After monitoring the phantom with the overlapping ROI at all couch locations it was found that the systematic offset measured with and without the mask were identical within 0.01cm at all couch locations (standard deviation of 0.0002). This would indicate that there is no appreciable difference in monitoring capabilities for AlignRT as a result of overlap with the masking material at any couch location over the full range of couch positions used for intracranial SRS treatments. This does not address the potential effects of patient motion under the mask causing issues with monitoring due to only portions of the ROI moving (e.g. patient surface) relative to the mask. It is therefore still recommended that the mask be taken out of the ROI for clinical cases until this effect can be further evaluated under controlled conditions.

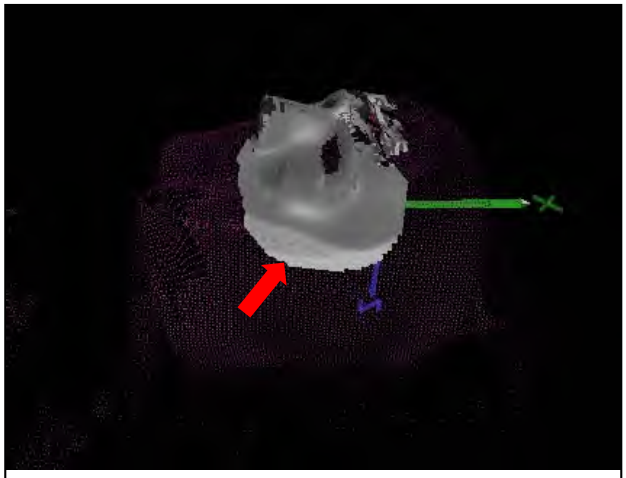

Figure 8: Image showing ROI transfer to both MAX-HD surface and the immobilizing mask.

Statistical Tolerance Prediction

After statistical evaluation of all of the results it was determined that the AlignRT SGRT system is in fact statistically capable of both localizing and/or monitoring patients to hold them within the industry standard tolerance of 1mm/0.5 degrees for intracranial SRS cases. Its capability to do so spans the full mechanical range of a modern linear accelerator and is capable of compensating for obstructions of the cameras as well as a full range of possible anatomical positions.

The data collected with the MAX-HD has shown that SGRT systems should be evaluated using phantoms with proper anatomical features that represent the full extent of the operational space with which the SGRT system will be asked to perform in order to determine if the system can maintain the tolerances required over that full operational space. The repeatability of the data over many days and weeks of measurement suggest that a tolerance set for clinical cases can be statistically characterized using an anthropomorphic phantom such as the MAX-HD. This tolerance set could potentially be enforced using a run statistic with predetermined upper and lower control limits. To test this theory the MAX-HD was fused to a clinical patient's anatomy prior to treatment using a best fit approach ensuring the head tilt and anatomical location of the isocenter was comparable between the patient anatomy and the MAX-HD anatomy. The patient's treatment plan was then transfer to the MAX-HD for statistical evaluation of the tracking capabilities of the AlignRT system under treatment conditions. The MAX-HD was then localized using the CBCT from the QA plan and a reference surface acquired using a duplicate of the patient's plan in AlignRT to confirm the ROI propagated to the MAX-HD was identical to the one being used for treatment. Once the reference surface was acquired the MAX-HD was monitored and treated exactly as the patient would be treated on the day of treatment while the real-time delta data was being recorded. Figure 9 is a plot of the magnitude of the measured displacement vector vs. time for the QA session on the MAX-HD.

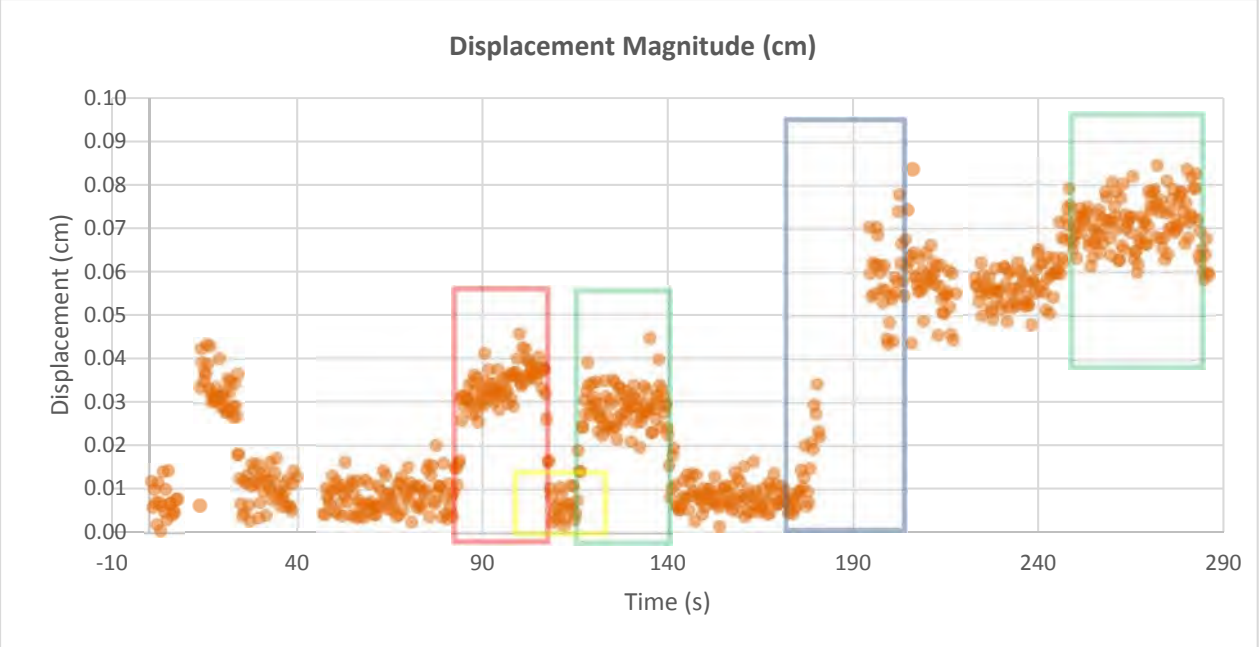

Figure 9: Real-time delta values obtained using the MAX-HD as a surrogate for the patient. Red box shows region of where camera pod 2 is obstructed. Yellow box shows where gantry head is up and all cameras are again unobstructed. Green boxes show region where camera pod 1 is obstructed during beam 1 and beam 2 deliveries. Blue box shows couch rotation moving from first arc to second arc delivery location.

With the QA complete the patient was brought in for treatment and the real-time delta values were recorded during the patient treatment. Once the treatment was completed the values for the magnitude of the treatment displacements were extracted and then correlated and matched in time to the QA measurements with the MAX-HD using an in-house software. Figure 10 below shows the result of the overlay between the QA real-time deltas (orange) and the actual real-time deltas (blue) from the patient's treatment.

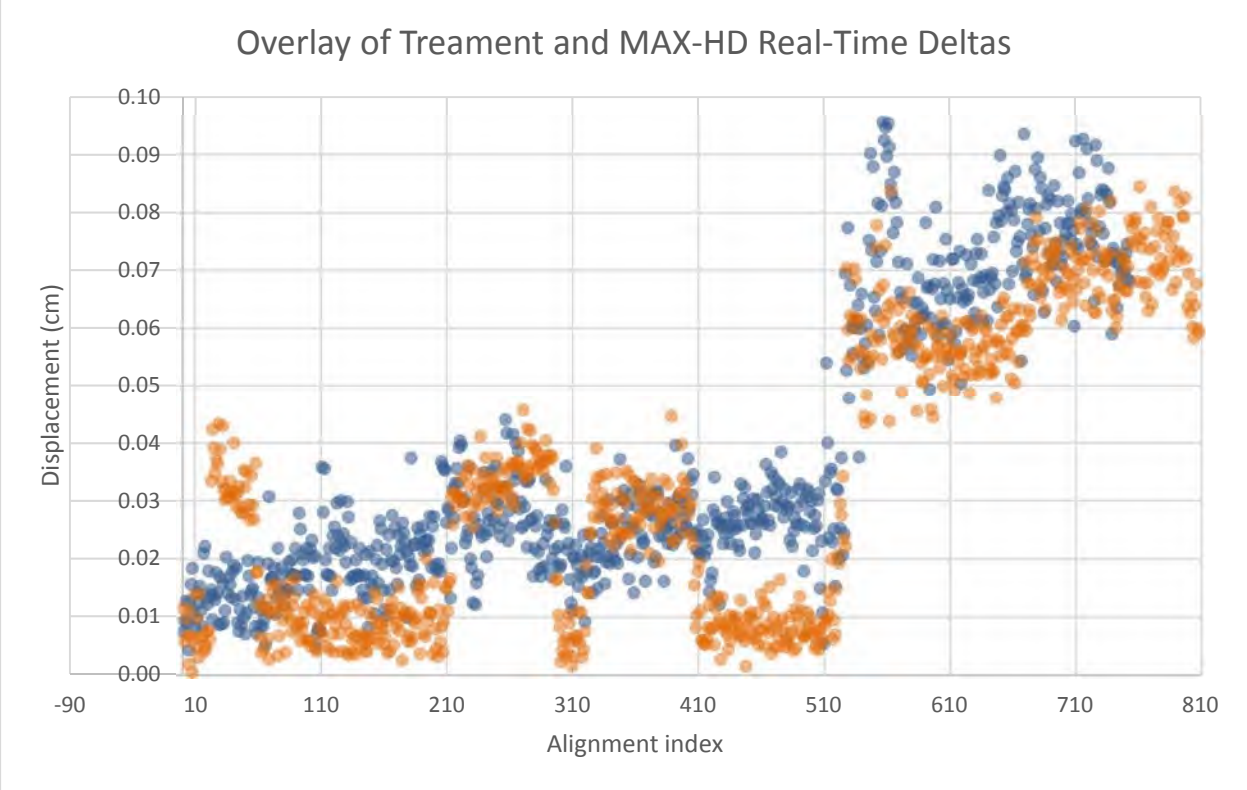

Figure 10: Real-time delta values obtained using the MAX-HD as a surrogate for the patient (orange) overlaid with the actual treatment real-time delta values (blue).

The above data shows, at least in concept, that dynamic run based statistics can be used to potentially predict specific table position based tolerances obtained during a QA evaluation of the patient plan using an anthropomorphic phantom like the MAX-HD. This potentially would allow clinicians to determine in real time if the displayed deviation is an expected or predictable fluctuation based on obstruction of a camera pod, a consequence of the table position, potential limitation of the field of view as defined by the imaging sensor, or an actual actionable deviation.

Conclusion

A systematic approach to testing an optical surface imaging system using both basic geometric based phantoms and a more sophisticated anthropomorphic phantom like the MAX-HD was presented. We were able to show that both CBCT and AlignRT under controlled phantom conditions were able to meet the TG-142 and TG-147 tolerance of <1mm for intracranial SRS localization verified through Winston-Lutz testing results. By systematically isolating various variables throughout the testing process we were able to show:

- The MAX-HD surface and the vendor supplied calibration phantom surface perform statistically the same (within random error) under various skin tone settings and monitoring conditions.
- Using an anthropomorphic phantom provides advantages over standard geometric phantoms by providing a basic anatomically defined operational space over which SGRT systems should be verified for performance.
- Location of isocenter relative to the monitoring surface can change the observable offset caused by camera obstruction.
- Anatomical orientation of the localization surface and location of isocenter relative to the monitoring surface does have an effect on the mean offset of the measurements within the 1mm/0.5degree tolerance window decreasing the amount of motion allowable before tolerance is exceeded.
- Isocenter placement within the cranial vault can result in table angles that should be avoided during treatment due to field of view limitations related to the imaging sensor size and camera orientation.
- AlignRT is capable of maintaining the TG-142, TG-147, and TG-135 specified tolerances for intracranial SRS over the full mechanical range of a modern linear accelerator and is capable of maintaining the accuracy required to alert operators of deviations outside of these tolerances
- Use of an anthropomorphic phantom like the MAX-HD in conjunction with an SGRT system like AlignRT can allow for future development of predictable and dynamic tolerances for SRS patients using run based statistics and control limits generated from a representative QA data set obtained during a phantom dry run.